# Predicting the Impact of Quenching on Mechanical Properties of Complex-Shaped Aluminum Alloy Parts

**D. D. Hall**
Graduate Research Assistant.

**I. Mudawar**
Professor and Director.

Boiling and Two-Phase Flow Laboratory,
School of Mechanical Engineering,
Purdue University,
West Lafayette, IN 47907

*The mechanical properties of age-hardenable aluminum alloy extrusions are critically dependent on the rate at which the part is cooled (quenched) after the forming operation. The present study continues the development of an intelligent spray quenching system, which selects the optimal nozzle configuration based on part geometry and composition such that the magnitude and uniformity of hardness (or yield strength) is maximized while residual stresses are minimized. The quenching of a complex-shaped part with multiple, overlapping sprays was successfully modeled using spray heat transfer correlations as boundary conditions within a finite element program. The hardness distribution of the heat-treated part was accurately predicted using the quench factor technique; that is, the metallurgical transformations that occur within the part were linked to the cooling history predicted by the finite element program. This study represents the first successful attempt at systematically predicting the mechanical properties of a quenched metallic part from knowledge of only the spray boundary conditions.*

## Introduction

Aluminum alloys are used for a wide range of applications, from common household products such as storm-screen window frames to structural members in military and commercial aircraft. The competitiveness of the global marketplace requires that heat-treated alloys satisfy stringent metallurgical requirements. The mechanical and metallurgical properties of extrusions and forgings of age-hardenable aluminum alloys are critically dependent on the rate at which the part is cooled (quenched) after the forming operation. If the final product does not meet the required specifications, a costly posttreatment operation is required, consisting of additional heat treatment and mechanical straightening of warped sections. In addition, the effect of posttreatment operations on the final metallurgical properties can seldom be predicted with accuracy. Thus, an intelligent spray quenching system is proposed that will optimize the quenching process to achieve superior part quality and consistency between production runs with minimal cost.

Spray quenching involves directing high-pressure sprays of liquid onto areas of the part where higher cooling rates are required. The droplets within the spray impact the part surface and remove heat very efficiently. Fairly uniform cooling of the part can be achieved by proper location and operation of the spray nozzles. Currently, the initial nozzle placement and operating pressure is one of trial and error, guided by the visual appearance of the part and the experience of the operator. Improper placement and operation of the nozzles may result in high residual stresses, nonuniform properties, low corrosion resistance, warping, soft spots, and cracking, all of which may lead to low strength and premature part failure. The nozzle configuration is subsequently modified until post-heat treatment tests reveal that the required mechanical and metallurgical properties were obtained.

The present study is part of an ongoing cross-disciplinary initiative at the Purdue University Boiling and Two-Phase Flow Laboratory involving several engineering departments, whose primary goal is the development of the CAD-based intelligent spray quenching system proposed by Deiters and Mudawar (1989) and illustrated in Fig. 1. The operator would input the composition and geometry of the extrusion or forging into the CAD system and, after consulting its extensive data bases, the system would output the nozzle configuration (type, placement, and pressure) required to achieve optimum cooling and the desired mechanical and metallurgical properties, thus eliminating the need for costly posttreatment operations. The specific objective of the present study is the following: predict the hardness distribution of a heat-treated Al 2024-T6 extrusion using the finite element method and compare with measurements in order to demonstrate that it is possible to configure a quenching system that would yield the desired product specifications without costly testing.

**Metallurgical Aspects of Heat Treatment.** The present study deals with heat-treatable aluminum–copper alloys, specifically Al 2024, which is composed of 93.5 percent aluminum, 4.4 percent copper, 1.5 percent magnesium, and 0.6 percent manganese. The development of the alloy microstructure during the heat treatment process can be more easily described by considering a two-component alloy consisting of aluminum and copper. Figure 2 shows the aluminum-rich region of the aluminum-copper phase diagram and the approximate composition range of the 2××× series of aluminum alloys (indicated by the shaded region), which are characterized by their ability to be significantly strengthened by artificial aging (precipitation hardening). The evolution of the alloy microstructure during slow cooling can be analyzed using phase diagrams, which represent the equilibrium phases associated with various combinations of temperature and composition. However, during the quenching process, phase transformations are time dependent and phase diagrams only serve as a general guide to understanding the heat treatment process.

The heat treatment process begins by heating the alloy to the solution heat treatment temperature, which is above the solvus temperature (the point where copper becomes soluble within aluminum) but below the solidus temperature (the point where the alloy begins to melt, complete melting occurs at the liquidus

Contributed by the Heat Transfer Division for publication in the JOURNAL OF HEAT TRANSFER. Manuscript received by the Heat Transfer Division March 1994; revision received July 1994. Keywords: Boiling, Materials Processing and Manufacturing Processes, Sprays/Droplets. Associate Technical Editor: A. Faghri.

temperature). When held above the solvus temperature for sufficient time, the copper (solute) will diffuse completely into the aluminum (solvent) to form a solid solution. Subsequent cooling of the alloy below the solvus temperature causes the solid solution to become supersaturated and the alloy seeks equilibrium by precipitating the $\theta$-phase, $CuAl_2$. As illustrated in Fig. 2, rapid cooling suppresses precipitation, preserving the homogeneous supersaturated solid solution, and results in an alloy that is age-hardenable. Conversely, slow cooling causes coarse precipitates to form at the grain boundaries and produces an alloy that cannot be age-hardened. Aging the alloy at an intermediate temperature allows the formation of a fine dispersion of precipitates within the aluminum grains, which hinders deformations and consequently increases the strength and hardness of the alloy. If the precipitates begin to coalesce into a more coarse dispersion, the alloy is overaged and there will be a smaller number of dislocation barriers, thus reducing strength and hardness.

From an age-hardenability viewpoint, it seems desirable to cool the entire part as quickly as possible from the solution heat treatment temperature. However, very rapid quenching of the exterior of a part having a cross section with large variations in thickness causes the interior of thin sections to cool much quicker than the interior of thick sections. Large spatial temperature gradients will exist during cooling, which lead to high thermal stresses and, hence, residual stresses and possible warping (if the part is relatively thin and the gradients are severe). If the part is cooled too slowly, uniform cooling may exist, but the desired strength or hardness cannot be obtained in the subsequent age-hardening heat treatment. Consequently, an optimum cooling strategy exists within a window of acceptable cooling rates such that the part is cooled as quickly and uniformly as possible (Chevrier et al., 1981). The proper placement and operation of spray nozzles allows the local surface heat flux to be controlled such that all locations within the part cool at an optimum rate. Before the tradeoff between maximizing strength and minimizing residual stresses can be analyzed, the quality of the quenching process must be quantified.

**C-Curve.** Fink and Willey (1948) pioneered the attempt to describe the relationship between cooling rate (quenching rate) and final alloy strength by identifying the temperature range over which the cooling rate has its most critical influence on the mechanical properties of the aged material. Their research resulted in the development of the C-curve, which represents the time required at different temperatures to precipitate a sufficient amount of solute to reduce the maximum attainable strength or hardness by a given percentage. Fink and Willey used a delayed quenching technique to determine the C-curve for rolled and extruded Al 7075-T6. Small samples, which could be considered isothermal at any given time, were rapidly quenched from the solution heat treatment temperature to intermediate temperatures where they were held for a given time and then rapidly quenched to room temperature. The samples were then artificially aged as specified by the temper designation and their yield strength, tensile strength, or hardness were measured. This procedure was repeated using different intermediate temperatures and different holding times. The locus of points on temperature–time coordinates with a particular hardness or strength defines a C-curve for the alloy. Evancho and Staley (1974) and Staley (1987) used transformation rate equations developed by Cahn (1956a) to derive a theoretical equation for the C-curve,

$$C_t = -k_1 k_2 \exp\left(\frac{k_3 k_4^2}{RT(k_4 - T)^2}\right) \exp\left(\frac{k_5}{RT}\right), \qquad (1)$$

where $C_t$ is the critical time required at a temperature, $T$, to precipitate a sufficient amount of solute to reduce the maximum attainable strength or hardness by the percentage represented by the C-curve. $k_1$ is the natural logarithm of the fraction of solute not precipitated or, as will be seen later, the yield-strength ratio or hardness ratio. The C-curve constants for Al 2024-T6 are $k_2 = 2.38 \times 10^{-12}$, $k_3 = 1.31 \times 10^3$, $k_4 = 8.40 \times 10^2$, and $k_5 = 1.47 \times 10^5$ (Kim, 1989).

The shape of the C-curve can be explained on the basis of the variation of nucleation and growth rates with temperature. At relatively high temperatures, the driving force for transformation is very small so that both nucleation rates (rate at which nuclei of a critical size or larger appear) and subsequent growth rates (rate of continued precipitation at nuclei above the critical size) are slow and a long time is required for transformation. At relatively low temperatures, slow diffusion rates (rate at which atoms cluster to form a nucleus) limit the rate of transformation. Therefore, a maximum precipitation rate is obtained at intermediate temperatures where diffusion rates remain high and the instability of the supersaturated solid solution causes high nucleation and growth rates.

Fink and Willey (1948) used average quenching rates through this critical temperature range to assess the quality of a quenching process. However, when cooling rates vary considerably during the quench (e.g., complex-shaped part), quantitative predictions of the final mechanical properties using average quenching rates were not possible. The quench factor technique developed by Evancho and Staley (1974) uses information from the entire C-curve to predict how the thermal history affects the final mechanical properties of wrought alloys.

**Quench Factor Technique.** A quench factor analysis of a transient nonisothermal quench is only valid if the internal re-

## Nomenclature

$c_p$ = specific heat at constant pressure
$C_t$ = critical time defined in Eq. (1)
$d_{32}$ = Sauter mean diameter (SMD)
$h$ = convection heat transfer coefficient
$h_{fg}$ = latent heat of vaporization
$H$ = Rockwell B hardness
$k$ = thermal conductivity
$k_1$ = natural logarithm of hardness ratio (or fraction of solute not precipitated) used to define the C-curve
$k_i$ = empirical constant in Eq. (1), $i$ = 2, 3, 4, or 5
$Nu_{32}$ = Nusselt number = $h\, d_{32}/k_f$
Pr = Prandtl number
$q''$ = heat flux
$Q''$ = volumetric spray flux
$R$ = universal gas constant = 8.314 J/gmol·K
$Re_{32}$ = Reynolds number = $\rho_f Q'' d_{32}/\mu_f$
$t$ = time
$T$ = temperature
$\Delta T$ = $T_s - T_f$
$\Delta T_{sub}$ = liquid subcooling = $T_{sat} - T_f$
$U_m$ = mean drop velocity
$x$ = coordinate along spray major axis
$y$ = coordinate along spray minor axis
$\zeta$ = fraction of solute precipitated during the quench
$\mu$ = dynamic viscosity
$\rho$ = density
$\sigma$ = yield strength; surface tension
$\tau$ = quench factor

### Subscripts

CHF = critical heat flux
DFB = departure from film boiling
$f$ = saturated liquid; final condition
$g$ = saturated vapor
$i$ = initial condition
max = maximum
min = minimum
MIN = minimum heat flux
OSP = onset of single-phase cooling
$s$ = surface condition
sat = saturated condition

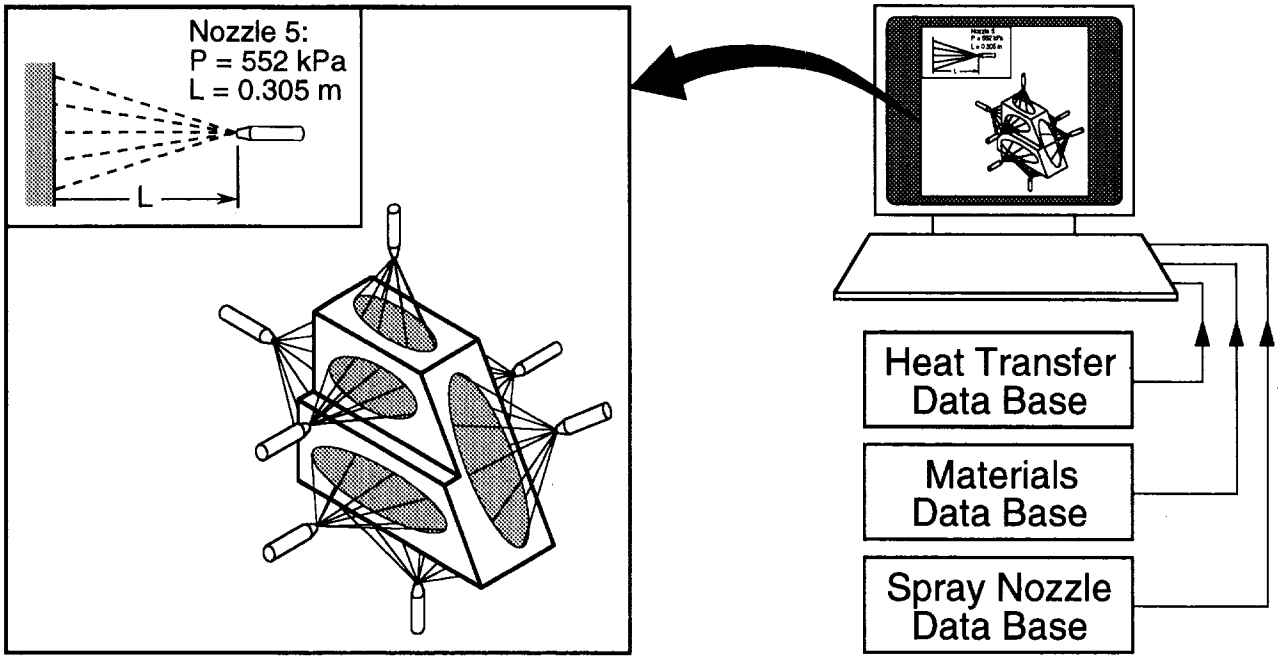


**Fig. 1 CAD-based intelligent spray-quenching system**

action (precipitation of solute), which occurs during cooling below the solvus temperature, is additive (Evancho and Staley, 1974). Avrami (1940) determined that a reaction is additive when the nucleation rate is proportional to the growth rate over the range of temperatures experienced during the reaction (i.e., precipitation kinetics remain unchanged). Cahn (1956b) demonstrated that additivity, as defined by Avrami, is observed in a reaction where the precipitation rate is only a function of temperature and amount of phase transformation previously completed. Furthermore, Cahn showed that a measure of the amount transformed during continuous cooling is given by

$$\tau = \int_{t_i}^{t_f} \frac{dt}{C_t}, \tag{2}$$

where $\tau$ was later referred to as the quench factor by Evancho and Staley (1974). Quench factors of zero and infinity correspond to suppression of precipitation and complete precipitation, respectively. The integral in Eq. (2) can be numerically calculated, as shown in Fig. 3, by discretizing the temperature–time cooling curve into small time increments. Each incremental quench factor represents the ratio of the amount of time the alloy was at a specific temperature to the amount of time required to obtain a specified amount of transformation at that temperature. As the time increment is decreased, the nonisothermal quench will essentially become a series of isothermal quenches, which are additive if the alloy obeys the rule of additivity over the entire range of transformation temperatures. In the process of determining the C-curve for Al 2024, Kim (1989) verified the assumption of additivity for this alloy.

Evancho and Staley (1974) developed the following equation to describe the precipitation kinetics of aluminum alloys during continuous cooling:

$$\zeta = 1 - \exp(k_1\tau), \tag{3}$$

where $\zeta$ equals the fraction of solute precipitated and $k_1$ corresponds to the C-curve from which the quench factor was calculated. Evancho and Staley (1974) and Staley (1987) developed the following equation to predict yield strength, $\sigma$, using Eq. (3) under the premise that the relative strength of age-hardenable aluminum alloys is directly related to the amount of solute remaining in solid solution $(1 - \zeta)$ after the quench (Conserva and Fiorini, 1973),

$$\frac{\sigma - \sigma_{\min}}{\sigma_{\max} - \sigma_{\min}} = \exp(k_1\tau), \tag{4}$$

where $\sigma_{\max}$ and $\sigma_{\min}$ are the maximum and minimum yield strengths of age-hardened specimens, which have been cooled from the solution heat treatment temperature at a near-infinite and extremely slow rate, respectively.

Axter (1980) performed various quenching experiments and concluded that the resistance to indentation, hardness, was proportional to yield strength for high strength aluminum alloys. The relative ease of measuring hardness prompted Bates (1988) and Kim (1989) to define a hardness ratio that would replace the yield strength ratio in Eq. (4),

$$\frac{H - H_{\min}}{H_{\max} - H_{\min}} = \exp(k_1\tau). \tag{5}$$

where $H_{\max}$ = 78.4 HRB and $H_{\min}$ = 2.2 HRB (Kim, 1989).

Thus, given the temperature–time history and C-curve of a wrought alloy, the final mechanical properties (strength or hardness) of the part can be determined using the quench factor technique. The quench factor technique has been successfully used to predict the yield strength and hardness of small (i.e., isothermal) aluminum alloy parts (Evancho, 1973; Evancho and Staley, 1974; Sawtell, 1984; Bates, 1987; Bates and Totten, 1988; Kim, 1989) and steel parts (Bates, 1988; Bates and Totten, 1992).

## Experimental Methods

**Materials Processing Test Bed.** The materials processing test bed shown in Fig. 4(*a*) was used to simulate the heat treatment process (solution heat treating, spray quenching, and artificial aging) of aluminum alloys in an industrial environment. The testpiece was heated in a Lindberg model 54857-V tube furnace having a cylindrical heating length of 60 cm and diameter of 15 cm. A three-zone programmable controller was used to control temperature of the three independent heating zones, thus ensuring uniform heating of the test piece. The furnace was mounted above the quench tank to allow the test piece to be

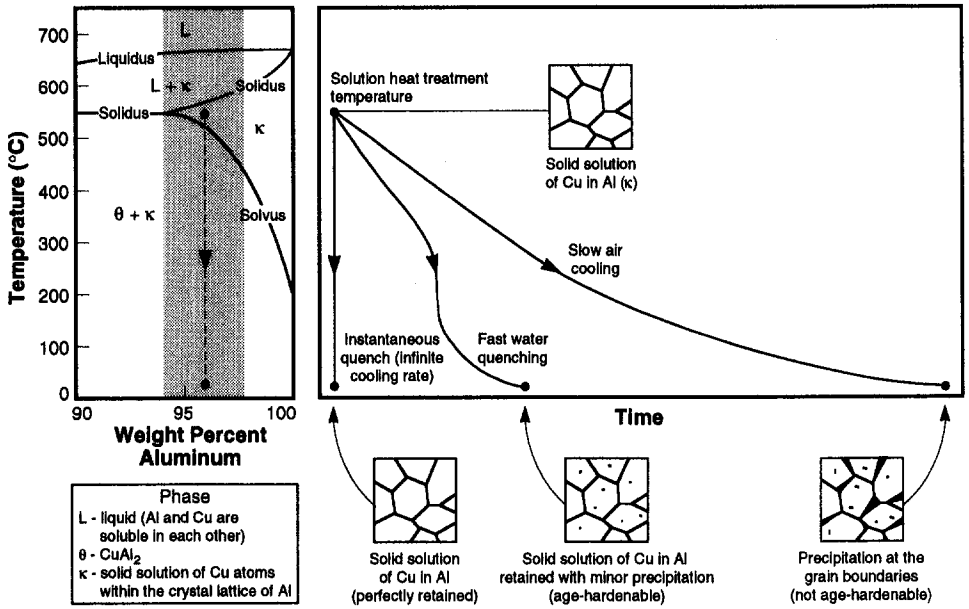


**Fig. 2 Aluminum-rich region of the Al–Cu phase diagram and the microstructure that develops following quenching of an Al–Cu (4.4 wt%) alloy**

lowered into the spray chamber using a vertical translation system. The spray chamber was fabricated from optical grade Lexan sheet to permit observation of the spray quenching process. Steam produced by the quench was removed by an exhaust system connected to the back of the test chamber. The lower quench tank served as a storage reservoir for recirculation of water during the quench. The fluid delivery loop contained a fan-cooled centrifugal pump, rated to deliver $25.2 \times 10^{-3}$ m$^3$/s (40 gpm) at 690 kPa (100 psi), and a 5 $\mu$m filter. The large capacity of the pump required a bypass line back into the quench tank to maintain flow stability.

Water was delivered to the spray nozzles using four nozzle arrays, one on each side of the spray chamber. The nozzle arrays, which consisted of three nozzles vertically separated by 11.4 cm (4.5 in.), allowed some flexibility of nozzle positioning relative to the test piece. The operating pressure of each nozzle array was independently controlled using four globe valves connected to four steel-reinforced flexible rubber hoses. Pressure was moni-

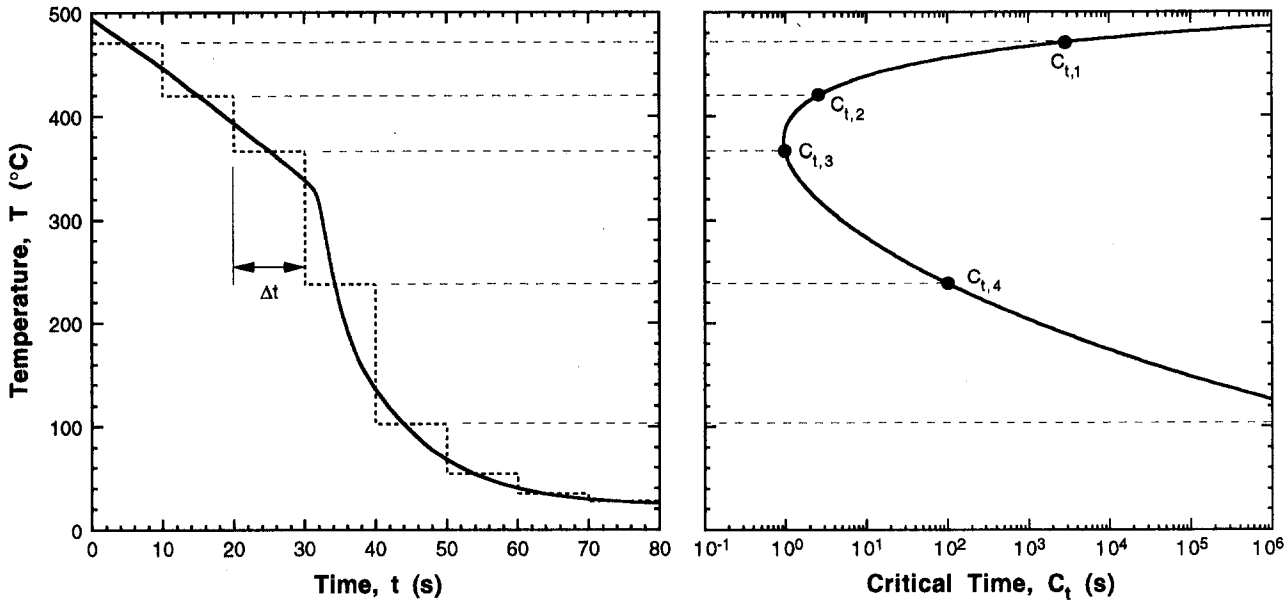


$$\tau = \int_{t_i}^{t_f} \frac{dt}{C_t} \approx \frac{\Delta t_1}{C_{t,1}} + \frac{\Delta t_2}{C_{t,2}} + \cdots + \frac{\Delta t_n}{C_{t,n}} = \sum_{m=1}^{n} \frac{\Delta t_m}{C_{t,m}} \quad \text{where} \quad C_t = -k_1 k_2 \exp\left(\frac{k_3 k_4^2}{RT(k_4 - T)^2}\right) \exp\left(\frac{k_5}{RT}\right), \ T \text{ in Kelvins}$$

$$H = H_{min} + (H_{max} - H_{min}) \exp(k_1 \tau)$$

**Fig. 3 Numerical calculation of the quench factor and hardness using a temperature–time curve and the C-curve**

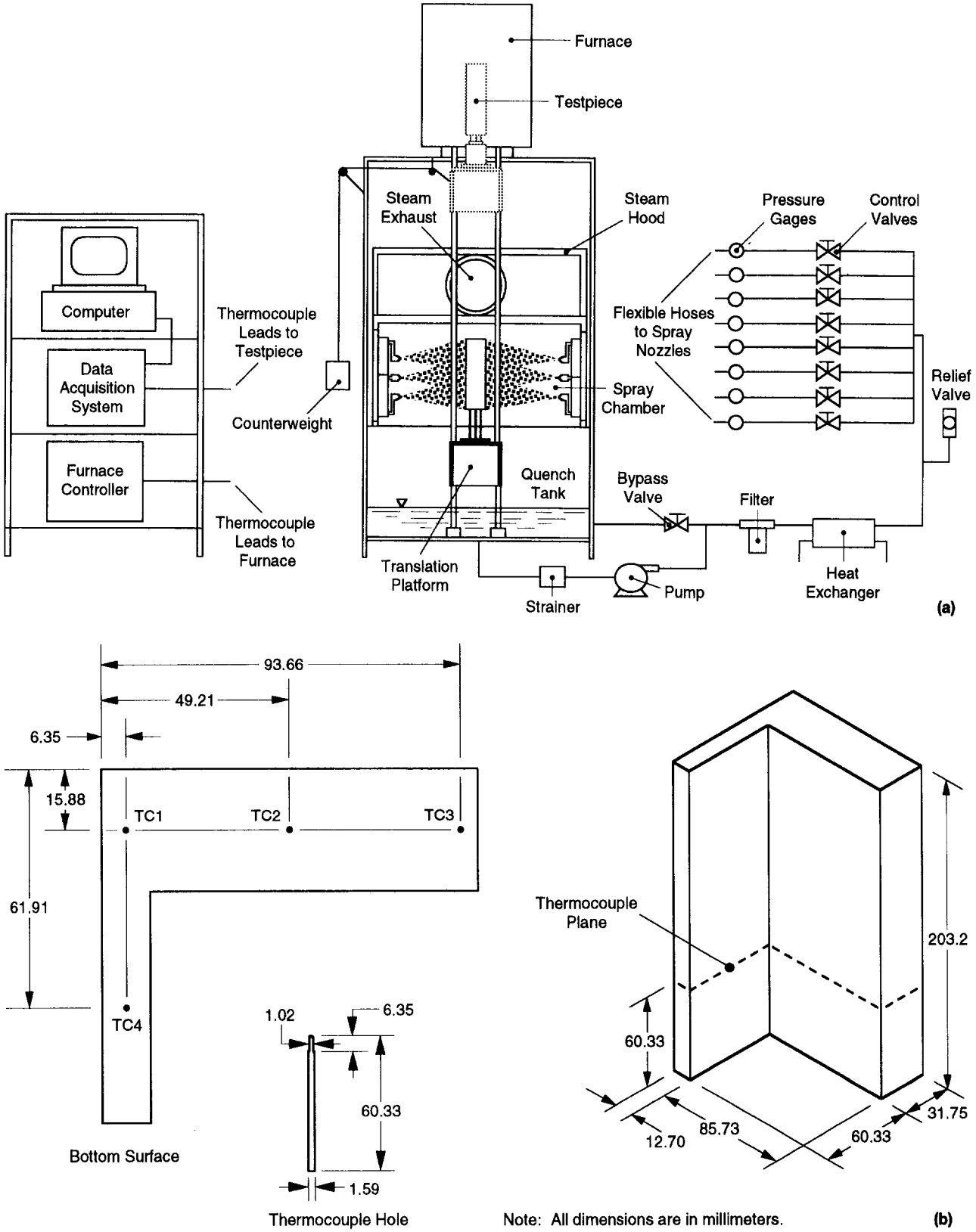


**Fig. 4** *(a)* **Schematic of the materials processing test bed;** *(b)* **Al 2024 L-shape dimensions and thermocouple placement**

tored using glycerin-filled stainless steel pressure gages with a range of 0–1.10 MPa (0–160 psi). The flat spray nozzles used in the present study were operated at a pressure of 552 kPa (80 psig) and a distance of 0.305 m (12 in.) from the test piece surface.

**L-Shaped Test Piece.** The L-shaped test piece shown in Fig. 4(*b*) was machined from an Al 2024 extrusion obtained from the Aluminum Company of America (ALCOA). The dimensions were chosen such that the effects of section thickness on cooling uniformity could be investigated both experimentally and nu-

merically. The thick and thin protruding sections had a thermal mass ratio of 4:1. The L-shape was instrumented with four chromel-alumel (type K) thermocouples, which consisted of 0.13 mm (0.005 in.) wire within a 0.81 mm (0.032 in.) diameter Inconel 600 sheathing with magnesium oxide insulation. The thermocouples were located such that the thermal history of the interior of both the thick and thin sections was fully characterized. Boron nitride powder, which has a thermal conductivity comparable to aluminum, was used to fill the void surrounding the thermocouple bead, thus ensuring excellent thermal contact with the alloy. Type K thermocouples were chosen for their high-temperature capabilities and adequate transient response. All thermocouples were placed in a plane three-tenths the length of the L-shape above the lower surface.

Surface roughness effects on the temperature-time history of spray quenched parts were observed by Rozzi (1991). Furthermore, Mudawar and Valentine (1989) and Klinzing et al. (1992) used polished surfaces to obtain the spray quenching heat transfer correlations used in the present numerical study (see Table 1). Therefore, the surface of the testpiece was carefully polished before each test to ensure uniform surface roughness and repeatability between quenches.

**Procedure.** The time the alloy is held at the solution heat treatment temperature depends upon the type of product, alloy composition, fabricating procedure, and section thickness. The extruded Al 2024 L-shape was heated to the solution heat treatment temperature of 495°C and held for 160 min before rapid quenching to room temperature. The subsequent artificial aging process resulting in the T6 temper consisted of 16 hr at 190°C (ASM, 1991).

Testing commenced with the raising of the test piece into the furnace using the vertical translation system. Accurate control of the furnace temperature was essential since the solution heat treatment temperature was only 7°C below the solidus temperature. When the test piece reached the solution heat treatment temperature (or artificial aging temperature), its temperature was constantly monitored to avoid overheating. The spray quenching process was initiated by engaging the pump and allowing the sprays to reach hydrodynamic equilibrium. The test piece was quickly lowered into the spray chamber using the translation system and thermocouple temperatures were recorded every 0.1 seconds throughout the quench.

A Goko Seiki Works model 3R hardness tester was used to measure Rockwell B hardness according to ASTM Standard E

**Table 1 Spray-quenching heat transfer correlations**

| Quenching (Boiling) Regime | Correlation |
|---|---|
| Film Boiling Regime (Klinzing et al., 1992) | $q'' = 6.325\times10^{1}\,\Delta T^{1.691}\,Q''^{0.264}\,d_{32}^{-0.062}$ |
| Point of Departure from Film Boiling (Klinzing et al., 1992) | $q''_{DFB} = 6.100\times10^{6}\,Q''^{0.588}\,U_m^{0.244}$<br>$\Delta T_{DFB} = 2.808\times10^{2}\,Q''^{0.087}\,U_m^{0.110}\,d_{32}^{-0.035}$ |
| Film-Wetting Regime (Klinzing et al., 1992) | $q'' = q''_{MIN} + \left(q''_{DFB} - q''_{MIN}\right)\left(\frac{\Delta T - \Delta T_{MIN}}{\Delta T_{DFB} - \Delta T_{MIN}}\right)^2$ |
| Point of Minimum Heat Flux (Klinzing et al., 1992) | $q''_{MIN} = 3.324\times10^{6}\,Q''^{0.544}\,U_m^{0.324}$<br>$\Delta T_{MIN} = 2.049\times10^{2}\,Q''^{0.066}\,U_m^{0.138}\,d_{32}^{-0.035}$ |
| Transition Boiling Regime (Klinzing et al., 1992) | $q'' = q''_{CHF} - \frac{q''_{CHF} - q''_{MIN}}{\left(\Delta T_{CHF} - \Delta T_{MIN}\right)^3}\left[\Delta T_{CHF}^3 - 3\,\Delta T_{CHF}^2\,\Delta T_{MIN} + 6\,\Delta T_{CHF}\,\Delta T_{MIN}\,\Delta T - 3\left(\Delta T_{CHF} + \Delta T_{MIN}\right)\Delta T^2 + 2\,\Delta T^3\right]$ |
| Point of Critical Heat Flux (Mudawar and Valentine, 1989) | $\frac{q''_{CHF}}{\rho_g\,h_{fg}\,Q''} = 122.4\left[1 + 0.0118\left(\frac{\rho_g}{\rho_f}\right)^{1/4}\left(\frac{\rho_f\,c_{p,f}\,\Delta T_{sub}}{\rho_g\,h_{fg}}\right)\right]\left(\frac{\sigma}{\rho_f\,Q''^2\,d_{32}}\right)^{0.198}$<br>$\Delta T_{CHF} = 18.0\left[\left(\rho_g\,h_{fg}\,Q''\right)\left(\frac{\sigma}{\rho_f\,Q''^2\,d_{32}}\right)^{0.198}\right]^{1/5.55}$ |
| Nucleate Boiling Regime (Mudawar and Valentine, 1989) | $q'' = 1.87\times10^{-5}\left(\Delta T\right)^{5.55}$ |
| Onset of Single-Phase Cooling (Mudawar and Valentine, 1989) | $\Delta T_{OSP} = 13.43\,Re_{32}^{0.167}\,Pr_f^{0.123}\left(\frac{k_f}{d_{32}}\right)^{0.220}$ |
| Single-Phase Regime (Mudawar and Valentine, 1989) | $Nu_{32} = 2.512\,Re_{32}^{0.76}\,Pr_f^{0.56}$ |

Units of the parameters: $q''$ (W/m$^2$), $\Delta T = T_s - T_f$ (°C), $Q''$ (m$^3$·s$^{-1}$/m$^2$), $U_m$ (m/s), $d_{32}$ (m), $h$ (W/m$^2$·K), $\rho_f$ (kg/m$^3$), $\rho_g$ (kg/m$^3$), $h_{fg}$ (J/kg), $c_{p,f}$ (J/kg·K), $k_f$ (W/m·K), $\mu_f$ (N·s/m$^2$), $\sigma$ (N/m)

Dimensionless parameters: $Nu_{32} = h\,d_{32}/k_f$, $Pr_f = c_{p,f}\,\mu_f/k_f$, $Re_{32} = \rho_f\,Q''\,d_{32}/\mu_f$

Range of validity of the correlations:

$T_f = 23$ °C, $Q'' = 0.58\times10^{-3} - 9.96\times10^{-3}$ m$^3$·s$^{-1}$/m$^2$, $U_m = 10.1 - 29.9$ m/s, $d_{32} = 0.137\times10^{-3} - 1.35\times10^{-3}$ m

Properties: The fluid properties used in the correlations for the point of incipient boiling and the single-phase regime are evaluated at the film temperature, $T_{film} = 0.5\,(T_s + T_f)$. The fluid properties used in the CHF correlation are evaluated at the fluid saturation temperature (Mudawar and Valentine, 1989).

18-93 (ASTM, 1993). Several external hardness measurements were conducted on the heat-treated test piece. Internal hardness measurements were subsequently obtained by cutting the test piece near the thermocouple plane using a wet band saw. The exposed surface was lightly milled, sanded, and polished to provide a smooth measurement surface. Lubricating oil was used during the milling process to eliminate heating of the test piece, which would possibly invalidate the measurements. The sanding and polishing processes removed material on the surface that was worked beyond its yield strength during the milling process.

## Numerical Methods

**Determination of the Heat Transfer Boundary Condition.** The spray quenching heat transfer correlations developed by Mudawar and Valentine (1989) and Klinzing et al. (1992), shown in Table 1, depend on values of the spray hydrodynamic parameters (volumetric spray flux, mean drop diameter, and mean drop velocity) just prior to impingement upon the surface. Hence, accurate knowledge of the spatial distribution of the spray hydrodynamic parameters was essential if the spray quenching process was to be numerically modeled. The spray hydrodynamic parameters of the nozzles used in the materials processing test bed were measured at discrete locations within the spray field and mathematical models of the spatial distributions were developed.

Flat spray nozzles are commonly used in spray quenching since they can provide relatively even spray coverage when several nozzles with overlapping spray patterns are utilized. The elliptical spray pattern generated by the flat spray nozzles facilitated the identification of major ($x$ axis) and minor ($y$ axis) spray axes. Visual examination of a typical flat spray nozzle revealed a uniform spray pattern, which was fairly symmetric about the major and minor axes.

The volumetric spray flux, $Q''$, was defined as the local volume flow rate per unit surface area. Measurements revealed that the volumetric spray flux exhibited a maximum value near the center of the spray and decayed exponentially away from the center. Thus, the spatial distribution of the volumetric spray flux was modeled by

$$Q'' = A_0 \exp(A_1 x^2 + A_2 y^2), \qquad (6)$$

where $A_0$ is the volumetric spray flux measured at the nozzle centerline and $A_1$ and $A_2$ are constants determined using a least-squares curve fit. The volumetric spray flux model for the flat spray nozzles used in the present study is illustrated in Fig. 5. A repeatability study was also conducted to verify that the models developed using a single nozzle were applicable to all nozzles of that type (Hall, 1993).

The spray quenching heat transfer correlations contain mean drop diameters and velocities instead of the complete drop size and velocity distributions of the spray. Sauter mean diameter, SMD or $d_{32}$, is the diameter of the drop whose ratio of volume to surface area is the same as that of the entire spray. The mean drop velocity, $U_m$, is simply the average of measured individual drop velocities. A phase-Doppler particle analyzer, manufactured by Aerometrics, Inc., was used to measure drop size and velocity simultaneously at discrete locations within the spray field. Multiple tests were conducted at each location to ensure repeatability. Several locations within the spray field were targeted in order to obtain a result that was representative of the entire spray. $d_{32}$ and $U_m$ did not appear to vary considerably, or predictably, between measurement locations. Hence, an average $d_{32}$ (286 $\mu$m) and an average $U_m$ (13.5 m/s) were used as the mathematical models for the spray field at a distance of 0.305 m (12 in.) from the nozzle orifice.

Typically, the quenching phase of a heat treatment operation consists of either a stationary part or a long extrusion moving through an array of overlapping sprays. The nozzle spacing should be optimized to eliminate undesired axial nonuniformity in the heat transfer coefficient. Volumetric spray flux appeared to be the primary spray hydrodynamic parameter controlling the spatial variation of the heat transfer coefficient since $d_{32}$ and $U_m$ were insensitive to location. Thus, an optimal nozzle configuration should produce a uniform spray field as well. The spray interaction between adjacent nozzles whose major axes coincide was investigated and a methodology was developed for optimizing nozzle spacing and adapting the single nozzle models for use with nozzle arrays having overlapping spray patterns (Hall, 1993). Figure 6 compares the nonoptimized nozzle configuration used in past studies to the nozzle configuration used in the present study, which eliminates the majority of axial temperature gradients in a stationary test piece and permits the quenching process to be analyzed using a two-dimensional numerical model.

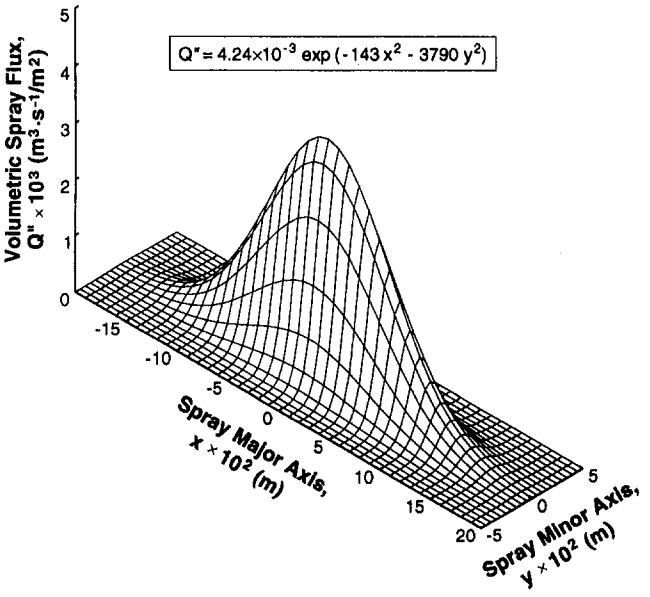


**Fig. 5 Spatial distribution model of volumetric spray flux for the flat spray nozzles used in the present study**

**Numerical Procedure.** Numerical simulation of the spray quenching process involves the solution of the transient heat diffusion equation with temperature dependent thermophysical properties and temperature and spatially dependent boundary conditions. The ability of the commercial finite element program ABAQUS (Hibbitt, Karlsson, and Sorensen, Inc., 1989) to define the heat transfer coefficient easily as a function of location and surface temperature made it ideal for the present study. The efficient nonlinear equation solver and self-adaptive time stepping scheme were additional benefits.

The spray quenching process will be optimized in future studies by adjusting the nozzle configuration; hence, locations on the surface of the extrusion may or may not be experiencing convection due to the water spray. Thus, the ABAQUS input file (Hall, 1993) was generalized to permit a convection boundary condition for all surface elements. A FORTRAN subroutine was written within the input file to determine the heat transfer coefficient as a function of surface temperature and surface location relative to the spray nozzles. The subroutine was consulted for each surface node at every iteration of every time increment. If the location was being sprayed, the subroutine performed the following tasks: (1) local spray hydrodynamic parameters were determined, (2) quenching regime experienced at this location, and (3) corresponding local surface heat flux were calculated using the spray quenching heat transfer correlations, and (4) convection heat transfer coefficient was defined as $h = q''/\Delta T$. Radiation heat transfer from sprayed surfaces was neglected since

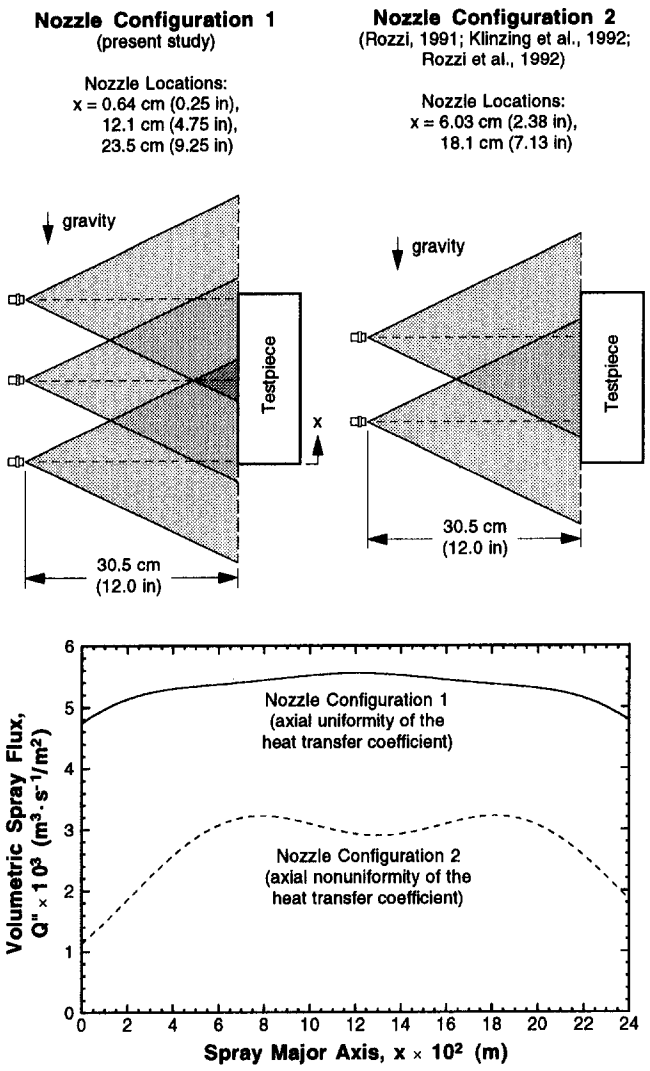


**Fig. 6 Spatial distribution of volumetric spray flux on the major axis of the nozzle configurations used in the materials processing test bed**

the heat transfer coefficient due to radiation alone (based on a surface temperature of 495°C and an emissivity of 0.15 (Gubareff et al., 1960)) was less than 0.6 percent of the lowest value of the heat transfer coefficient due to spray convection (determined using the film boiling correlation listed in Table 1 for a location near the edge of the spray field). Free convection and radiation from unsprayed surfaces were found to have a negligible effect on the numerical results. ABAQUS iterated each time increment until the solution at each node differed by less than 0.01°C between iterations. A nearly continuous temperature–time history was obtained by defining a maximum allowable time increment of 0.1 seconds. Solution convergence was investigated to determine the appropriate element type and size required by the present problem.

## Results and Discussion

**Experimental Results.** The nozzle configuration used in the quenching process was chosen such that axial uniformity and in-plane variations of hardness would be obtained in the heat treated part. The in-plane variations of hardness were necessary to verify that the quench factor technique accurately predicts the trends in hardness throughout the part cross section. Previous experiments indicated that a single nozzle array (consisting of three optimally spaced nozzles whose major axes coincide) impinging the thin section yielded the largest possible variation of in-plane hardness using this type nozzle and operating pressure (Hall, 1993). This realistic nozzle configuration was justified by viewing the L-shape as the symmetric fourth of an I-beam extrusion as shown in Fig. 7. The web thickness of an I-beam is usually less than the flange thickness. However, the thicker web used in the present study was necessary to promote in-plane hardness variations. The thermocouples were located within the L-shape such that relatively different cooling histories would be obtained and, hence, a wide range of hardness values would be predicted using the quench factor technique.

The L-shape was solution heat treated, spray quenched, and artificially aged to achieve the T6 temper. Rockwell B hardnesses predicted using the quench factor technique and temperatures measured during the spray quenching process are indicated in Fig. 8(*a*). Following artificial aging, several hardness measurements were made on the surface of the test piece near the thermocouple plane. The L-shape was subsequently cut open and the exposed surface carefully prepared for additional hardness measurements near the thermocouple locations. The measurements shown in Fig. 8(*a*) represent an average hardness rounded to the nearest 0.5 HRB. External measurements made near thermocouple locations were in good agreement with the quench factor predictions. The percent differences between predicted and externally measured hardness were 0.6, 3.3, and 0.7 percent for the surface locations near TC 1, TC 3, and TC 4, respectively. Additional measurements conducted on other planes parallel to the thermocouple plane confirmed the axial uniformity of hardness. The percent differences between predicted and internally measured hardness were 0.1, 1.0, 1.2, and 2.8 percent at TC 1, TC 2, TC 3, and TC 4, respectively.

The maximum attainable hardness for Al 2024-T6, $H_{max}$ in Eq. (5), may be approximately 2 HRB higher than the value used to predict hardness in the present study (Kim, 1989). Thus, hardness predicted using the quench factor technique has an uncertainty of approximately 2.5 percent. This uncertainty combined with the uncertainty associated with the calibration of the hardness tester explains any differences in magnitude between measured and predicted hardness. Furthermore, these uncertainties do not affect the hardness trends (measured or predicted) observed within the L-shape. Thus, the experimental hardness measurements verify that the quench factor technique accurately predicts the hardness distribution of a heat-treated part from its measured temperature-time history. This confirmation paves the way for the next phase leading to the development of the CAD-based intelligent spray quenching system: combine the quench factor technique and the finite element prediction of temperature history to predict hardness without any experimental data.

**Numerical Predictions.** The ability of the numerical methods developed in the present study to predict the temperature–time history of a spray-quenched part accurately was verified in a related study (Hall, 1993). The quench factor technique was

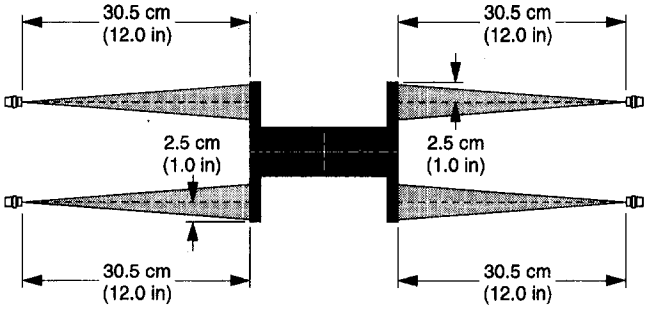


**Fig. 7 I-beam extrusion and possible nozzle configuration used in industry. The L-shape used in the present study represents the symmetric fourth of the I-beam.**

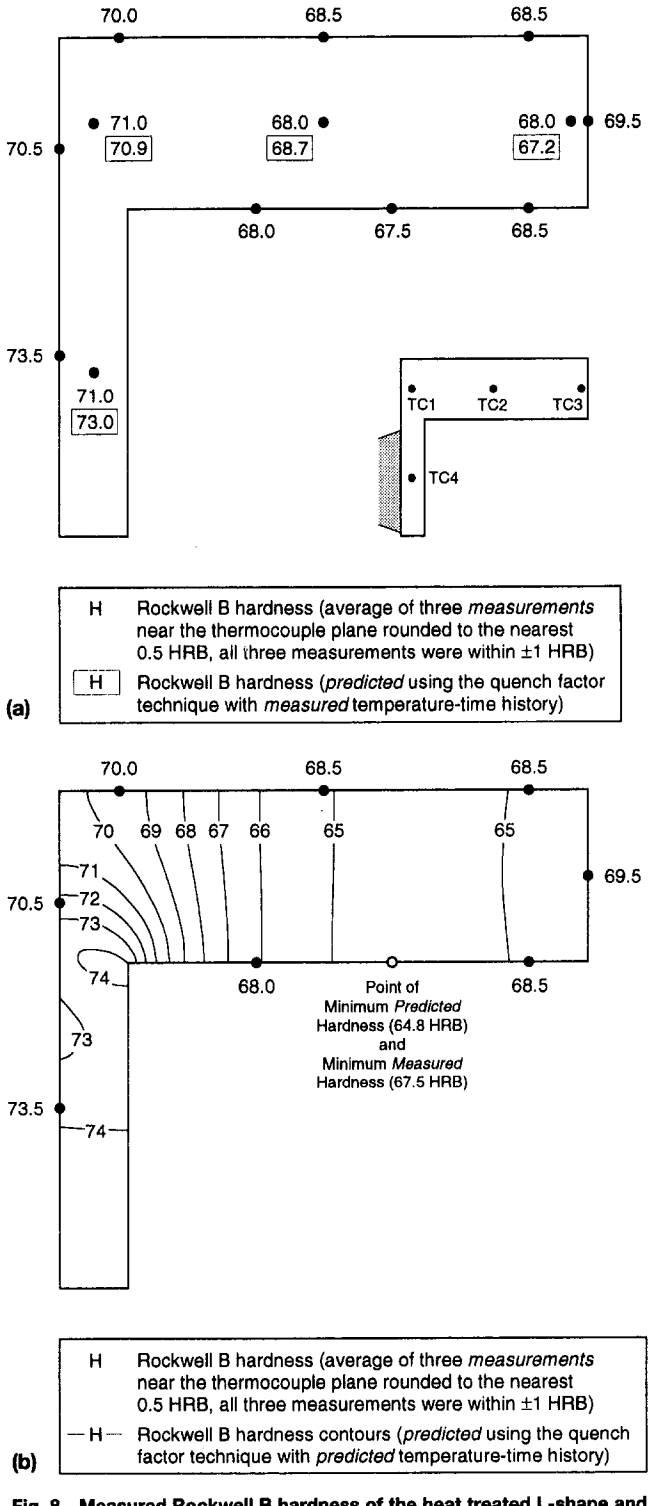


**Fig. 8 Measured Rockwell B hardness of the heat treated L-shape and hardness predicted using the quench factor technique with (*a*) measured and (*b*) predicted temperature–time history**

used in the current study to predict the hardness distribution from this temperature–time history. Figure 8(*b*) shows that external hardness measurements made on the surface of the test piece near the thermocouple plane were in good agreement with the numerical predictions. The predicted hardness distribution accurately represented the trends in hardness observed throughout the L-shape. Furthermore, the point of minimum predicted hardness and minimum measured hardness coincided. The difference between measured and predicted hardness was a maximum in the thick section. This was attributed to significant forced convection from unsprayed surfaces of the testpiece to mist and air currents inside the spray chamber. The methodology developed in the current study accounted only for free convection from unsprayed surfaces and, hence, the thick section cooled quicker and had a slightly higher hardness than predicted. This phenomenon did not affect the ability of the method to predict trends in hardness accurately. Furthermore, this error should decrease when a larger portion of the surface is being sprayed (i.e., as the quench is improved by adding sprays to the thick section).

The experimental hardness measurements verify that the quench factor technique accurately predicts the hardness of a heat-treated part from the temperature history predicted using the methodology developed in this study. This additional confirmation paves the way for the final phase leading to the development of the CAD-based intelligent spray-quenching system: optimization of the spray quenching process by predicting and testing more appropriate nozzle configurations to maximize the magnitude and uniformity of hardness. This issue will be addressed in future studies.

## Conclusions

This study continues the development of the CAD-based intelligent spray-quenching system, originally proposed by Deiters and Mudawar (1989), which, once completed, will optimize the quenching of aluminum alloys to achieve superior part quality. The primary goal of the present study was to develop a method for predicting the hardness distribution within heat-treated aluminum alloy extrusions. Key conclusions from this study are as follows:

1 Previously, the quench factor technique was applied only to small isothermal samples having simple geometries (e.g., spheres, sheet). This study has shown that the quench factor technique accurately predicts the hardness distribution of non-isothermal, complex-shaped aluminum alloy parts from the measured temperature–time history.

2 The spray quenching of a complex-shaped part with multiple, overlapping spray nozzles was successfully modeled using the methodology developed in the current study and the spray-quenching heat transfer correlations developed by Mudawar and Valentine (1989) and Klinzing et al. (1992). The hardness distribution of a heat-treated Al 2024-T6 extrusion was successfully predicted using the quench factor technique and the numerically predicted temperature–time history.

3 Since the quench factor technique has been validated for both strength and hardness, the methodology developed in this study should also give accurate yield strength predictions.

4 The coupling of the quench factor technique with the finite element method and spray-quenching heat transfer correlations enables the determination of the final mechanical properties a priori; hence, the performance of a spray quenching system can be judged prior to operation. Once perfected, the CAD-based intelligent spray quenching system will significantly reduce cost and increase productivity.

## Acknowledgments

The authors gratefully acknowledge the financial support of the Purdue University Engineering Research Center for Intelligent Manufacturing Systems. Financial support for the first author was provided in the form of the United States Department of Energy Predoctoral Integrated Manufacturing Fellowship. The authors also thank Jerry Hagers, Rudolf Schick, and Chris Schaffer of Spraying Systems Company and Gerry Dail of ALCOA for their valuable technical assistance.

## References

ASM, 1991, *ASM Handbook*, Vol. 4, 10th ed., ASM International, Materials Park, OH.

ASTM, 1993, *Annual Book of ASTM Standards,* Vol. 03.01, American Society for Testing and Materials, Philadelphia, PA.

Avrami, M., 1940, "Kinetics of Phase Change II—Transformation-Time Relations for Random Distribution of Nuclei," *Journal of Chemical Physics,* Vol. 8, pp. 212–224.

Axter, S. E., 1980, "Effects of Interrupted Quenches on the Properties of Aluminum," Society of Manufacturing Engineers Technical Paper CM80-409.

Bates, C. E., 1987, "Selecting Quenchants to Maximize Tensile Properties and Minimize Distortion in Aluminum Parts," *Journal of Heat Treating,* Vol. 5, pp. 27–40.

Bates, C. E., 1988, "Predicting Properties and Minimizing Residual Stress in Quenched Steel Parts," *Journal of Heat Treating,* Vol. 6, pp. 27–45.

Bates, C. E. and Totten, G. E., 1988, "Procedure for Quenching Media Selection to Maximize Tensile Properties and Minimize Distortion in Aluminum Alloy Parts," *Heat Treatment of Metals,* Vol. 15, pp. 89–97.

Bates, C. E., and Totten, G. E., 1992, "Application of Quench Factor Analysis to Predict Hardness Under Laboratory and Production Conditions," *Proceedings of the First International Conference on Quenching and Control of Distortion,* Chicago, IL, pp. 33–39.

Cahn, J. W., 1956a, "The Kinetics of Grain Boundary Nucleated Reactions," *Acta Metallurgica,* Vol. 4, pp. 449–459.

Cahn, J. W., 1956b, "Transformation Kinetics During Continuous Cooling," *Acta Metallurgica,* Vol. 4, pp. 572–575.

Chevrier, J. C., Simon, A., and Beck, G., 1981, "Optimal Cooling Rate and Process Control in Metallic Parts Heat Treatment," *Heat and Mass Transfer in Metallurgical Systems,* D. B. Spalding and N. H. Afgan, eds., Hemisphere Publishing Corp., Washington, DC, pp. 535–544.

Conserva, M., and Fiorini, P., 1973, "Interpretation of Quench-Sensitivity in Al-Zn-Mg-Cu Alloys," *Metallurgical Transactions,* Vol. 4, pp. 857–862.

Deiters, T. A., and Mudawar, I., 1989, "Optimization of Spray Quenching for Aluminum Extrusion, Forging, or Continuous Casting," *Journal of Heat Treating,* Vol. 7, pp. 9–18.

Evancho, J. W., 1973, "Effects of Quenching on Strength and Toughness of 6351 Extrusions," Alcoa Laboratories Report 13-73-HQ40, Alcoa Center, PA.

Evancho, J. W., and Staley, J. T., 1974, "Kinetics of Precipitation in Aluminum Alloys During Continuous Cooling," *Metallurgical Transactions,* Vol. 5, pp. 43–47.

Fink, W. L., and Willey, L. A., 1948, "Quenching of 75S Aluminum Alloy," *Transactions AIME,* Vol. 175, pp. 414–427.

Gubareff, G. G., Janssen, J. E., and Torborg, R. H., 1960, *Thermal Radiation Properties Survey,* 2nd ed., Honeywell Research Center, Minneapolis, MN.

Hall, D. D., 1993, "A Method of Predicting and Optimizing the Thermal History and Resulting Mechanical Properties of Aluminum Alloy Parts Subjected to Spray Quenching," M.S. Thesis, Purdue University, West Lafayette, IN.

Hibbitt, Karlsson and Sorensen, Inc., 1989, *ABAQUS User's Manual, Ver. 4.8,* Providence, RI.

Kim, J. S., 1989, "Prediction of the Influence of Water Spray Quenching on the Age-Hardenability of Aluminum Alloy 2024," M.S. Thesis, Purdue University, West Lafayette, IN.

Klinzing, W. P., Rozzi, J. C., and Mudawar, I., 1992, "Film and Transition Boiling Correlations for Quenching of Hot Surfaces With Water Sprays," *Journal of Heat Treating,* Vol. 9, pp. 91–103.

Mudawar, I., and Valentine, W. S., 1989, "Determination of the Local Quench Curve for Spray-Cooled Metallic Surfaces," *Journal of Heat Treating,* Vol. 7, pp. 107–121.

Rozzi, J. C., 1991, "Quenching of Aluminum Parts Having Irregular Geometries Using Multiple Water Sprays," M.S. Thesis, Purdue University, West Lafayette, IN.

Rozzi, J. C., Klinzing, W. P., and Mudawar, I., 1992, "Effects of Spray Configuration on the Uniformity of Cooling Rate and Hardness in the Quenching of Aluminum Parts With Nonuniform Shapes," *Journal of Materials Engineering and Performance,* Vol. 1, pp. 49–60.

Sawtell, R. R., 1984, "Effects of Quenching Path in Aluminum Alloy 7075," *Aluminum,* Vol. 60, pp. 198–202.

Staley, J. T., 1987, "Quench Factor Analysis of Aluminum Alloys," *Materials Science and Technology,* Vol. 3, pp. 923–935.